Comparison of Subsonic/Transonic Aftbody Flow Prediction Methods

Lawrence E. Putnam*
NASA Langley Research Center, Hampton, Virginia
and
James Mace†
Air Force Wright Aeronautical Laboratories, Dayton, Ohio

A comparison of computational methods used in the calculation of nozzle aftbody flows at subsonic and transonic speeds is presented. One class of methods reviewed are those which patch together solutions for the inviscid, boundary-layer, and plume flow regions. The second class of methods reviewed are those which computationally solve the Navier-Stokes equations over nozzle aftbodies with jet exhaust flow. Computed results from the methods are compared with experiment. Advantages and disadvantages of the various methods are discussed along with opportunities for further development of these methods.

Nomenclature

$C_{D,\beta}$ = boattail pressure drag coefficient
C_P = pressure coefficient
c_v = specific heat at constant volume
c_p = specific heat at constant pressure
D = maximum diameter of body
D_E = diameter of nozzle exit
d_B = diameter of nozzle base
E = mean total energy
J = transformation Jacobian
l = length of nozzle boattail
M = Mach number
NPR = ratio of nozzle total pressure to freestream static pressure
p = static pressure
p_t = total pressure
$p_{t,2}$ = impact pressure measured with a pitot tube
P_R = molecular Prandtl number
$P_{R,t}$ = turbulent Prandtl number
R = gas constant
Re = Reynolds number
r = radial distance
T = temperature
u, U = velocity in axial direction
v = velocity normal to axis
x = axial distance downstream of start of nozzle boattail
Δx = axial distance downstream of nozzle exit
y = general radial coordinate
z = general axial coordinate
α = angle of attack
γ = ratio of specific heats
δ = boundary-layer thickness
δ^* = boundary-layer displacement thickness
ϵ = turbulent eddy viscosity coefficient
θ = general angular coordinate
λ = constant in relaxation eddy viscosity model of Shang and Hankey
μ = laminar viscosity coefficient
ρ = density
τ = shear stress
ψ = stream function

Subscripts
e = edge
eff = effective
j = jet
sep = separation
∞ = freestream
$1,2$ = inner, outer mixing layer computational boundary

Presented as Paper 81-1694 at the AIAA Aircraft Systems and Technology Conference, Dayton, Ohio, Aug. 11-13, 1981; submitted Sept. 3, 1981; revision received May 17, 1982. This paper is declared a work of the U.S. Government and therefore is in the public domain.

*Assistant Head, Propulsion Aerodynamics Branch, Transonic Aerodynamics Division. Member AIAA.
†Aerospace Engineer, Flight Dynamics Laboratory. Member AIAA.

Introduction

FLOW over nozzle boattail configurations at subsonic and transonic speeds is dominated by strong viscous/inviscid interaction effects. As illustrated on Fig. 1, this flow is characterized by very thick boundary layers, strong pressure gradients which may cause the boundary layer to separate, a jet exhaust plume that may grow or diminish in size depending on nozzle pressure ratio, and a large viscous mixing region between the jet and external flow. If the flow is transonic, shock waves will also be present. Because of these strong viscous/inviscid interactions, inviscid theoretical methods have been found to be inadequate for predicting nozzle/aftbody flow. In the past, therefore, wind tunnel testing has been the primary means for determining afterbody drag as well as the detailed flow characteristics resulting from nozzle/aftbody interactions.

In recent years, a considerable effort has been underway to develop analytical procedures for predicting the drag and flow characteristics over nozzle/aftbodies. Primary emphasis to date has been directed at developing prediction techniques for uninstalled nozzle configurations at zero or low angles of attack. The procedures developed have included the following: 1) empirical methods for predicting nozzle pressure drag, 2) the patched inviscid/viscous interaction technique,[1-13] 3) the velocity-split method,[14] and 4) solutions of the Navier-Stokes equations.[15-25]

The purpose of the present paper is to assess the current status of the patched inviscid/viscous interaction technique and solutions of the Navier-Stokes equations for predicting

nozzle afterbody flow. No discussion of empirical methods or the velocity-split method will be provided. A detailed description of the axisymmetric patched inviscid/viscous interaction method of Wilmoth[4,10] will be given along with comparisons with experiment to indicate its capabilities. Results of a survey of Navier-Stokes solutions available in the open literature for nozzle flow will be discussed with special emphasis on the similarities and differences of these solutions. Typical results from Navier-Stokes solution codes will be presented to illustrate their capabilities. Finally, some discussion of future computational needs will be provided.

Discussion

Patched Inviscid/Viscous Interaction Method

The patched inviscid/viscous methods[1-13] that have been developed for predicting nozzle aftbody flows are limited to axisymmetric conditions. For this method, the flow about the nozzle boattail is subdivided into several regions (see Fig. 2). In general, these regions include 1) the essentially inviscid external flow, 2) the boundary-layer flow over the nozzle surfaces, 3) the essentially inviscid jet exhaust, and 4) the mixing layer between the jet exhaust and the external stream. In the various patched solutions available in the open literature, the boundary-layer growth effects on the nozzle external surfaces are generally modeled using an effective surface determined by the boundary-layer displacement thickness. Some researchers, however, have modeled this effect using a mass injection boundary condition.[13] Various approaches have been used to model the shear flow resulting from the mixing between the external stream and jet. Usually this effect has been modeled with an "effective body" concept whereby a displacement-thickness-like correction is applied to the inviscid jet boundary. In this manner both the jet plume entrainment and growth effects are included simultaneously in the solution. After subdividing the flow, each region is computed iteratively using whatever equation set and solution methodology the analyst deems appropriate. For example, the external flow could be computed using a linear panel method solution of the Laplace equations with a compressibility correction or it could be computed using a finite-difference solution of the nonlinear full potential flow equations. The boundary-layer equations can be solved using any of several integral techniques or with a finite-difference technique. Some researchers have used the inverse boundary-layer concept where a displacement thickness is specified and an edge velocity is computed to match with the external flow.[12,13] For the jet exhaust plume most researchers use a supersonic marching solution. Jet entrainment effects have been modeled in many ways, from simply setting the skin friction equal to zero in the boundary-layer solution to solving the parabolic shear layer equations.

The final ingredient in the patched solution is the scheme used to iterate between the solutions in the various flow regions. Generally the approach has been to use the pressures along the "effective" body as the matching parameter; that is, the external flow over the "effective" body is computed. The pressures from this solution are fed into the boundary-layer solution, jet exhaust flow solution, and jet-mixing layer solutions to provide a correction to the displacement surface. The updated "effective" body is then used for the next external flow calculation. Those researchers[12,13] who use the inverse boundary-layer approach assume a boundary-layer displacement surface, compute the edge velocities with both the external flow and viscous flow solutions, and then modify this displacement thickness by some relaxation scheme.

In general, the patched inviscid/viscous interaction methods available[1-13] all provide reasonable predictions of nozzle pressure distributions at subsonic and transonic speeds. The boattail pressure drag predicted by these methods vary considerably in accuracy. Wilmoth[4,10] has developed a patched method that provides very good predictions of nozzle surface pressure distributions, nozzle pressure drag, and nozzle flowfield characteristics. Wilmoth's method is also capable of predicting the effects of jet exhaust temperature, composition, and chemistry. This method has therefore been selected for further discussion to illustrate in some detail the patched technique.

Wilmoth subdivides the flow into the regions shown on Fig. 2. The inviscid external flow is solved using the South and Jameson relaxation solution for the transonic full potential flow equation.[26,27] Computation of the inviscid jet exhaust plume is accomplished using Dash's shock-capturing/shock-fitting solution of the Euler equations.[28] The boundary-layer flow over the nozzle external surface is computed using a modified Reshotko-Tucker integral solution.[29,30] In the event of boundary-layer separation, the procedure developed by Presz[8] is used. Presz uses a control volume procedure to determine the location of the separation point. Then, downstream of the separation point, a control volume technique is also used to determine the shape of the discriminating streamline that separates the reverse flow region from the outer flow. Once the discriminating streamline is determined, the boundary-layer displacement thickness computed by the boundary-layer solution is added.

The effect of the jet-mixing region is accounted for with the overlaid method of Dash and Pergament.[31,32] In this technique, after the external inviscid flowfield and the inviscid jet exhaust plume are computed, a viscous marching solution utilizing streamline coordinates is overlaid on these flowfields. At each longitudinal station an effective displacement thickness is computed. If the velocity of the jet is significantly larger than the external velocity, the "effective" plume boundary can be smaller than the inviscid jet boundary (i.e., a negative displacement thickness).

The final ingredient of the patched solution technique is the iteration scheme. The iteration procedure used by Wilmoth is

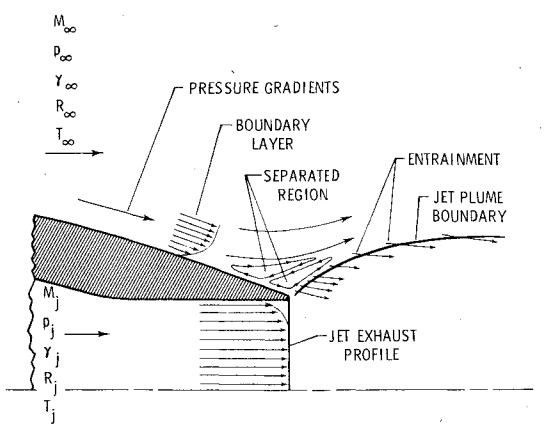

Fig. 1 Schematic of nozzle aftbody flow.

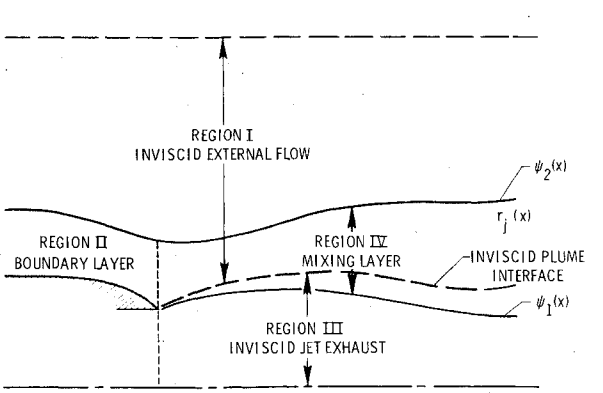

Fig. 2 Computational regions used in patched inviscid/viscous interaction technique.

as follows:

1) Calculate the inviscid external flow over the effective body (for the first iteration, this is the actual body with an assumed plume shape).

2) Calculate the boundary-layer displacement thickness using edge conditions from step 1.

3) Calculate the inviscid jet exhaust boundary and flowfield using pressure along boundary from step 1.

4) Calculate the flow in the mixing region using initial conditions from step 2, and the flowfields from steps 1 and 3.

5) Update the effective body shape using an under relaxation technique.

The procedure is repeated until convergence occurs. In general, convergence requires about ten viscous iterations for attached boundary-layer solutions and about 20 iterations for separated boundary-layer calculations. The computation typically takes about 30 CPU seconds per iteration on a CYBER 175 computer.

Calculations made by Wilmoth[10] are compared with experimental measurements[33] on Figs. 3-8. On Fig. 3, the effect of including the jet plume entrainment in the solution is illustrated. Here the pressure distribution over an $l/D=1.768$, $d_B/D=0.51$ circular arc boattail convergent nozzle operating at a nozzle pressure ratio (NPR) of 2 and at a freestream Mach number of 0.4 is shown. When the jet entrainment effect is neglected in the calculation, the theory overpredicts the pressures on the nozzle and underpredicts the drag. The addition of the jet entrainment effect results in a substantial improvement in the prediction accuracy. Note that the primary effect of jet entrainment is an increase in the entrainment velocity near the nozzle exit. The decay of this entrainment velocity with axial distance downstream of the nozzle exit is essentially the same as the case where entrainment is neglected.

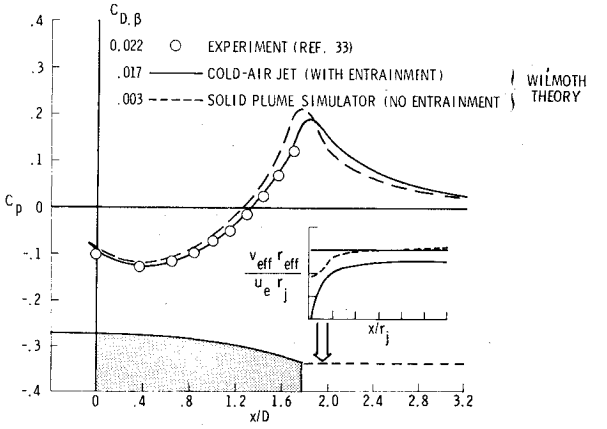

Fig. 3 Basic entrainment effect on nozzle boattail/jet interaction. $l/D=1.768$, $d_B/D=0.51$ circular arc nozzle at $M_\infty=0.4$ and NPR = 2.0.

Figure 4 shows the capability of Wilmoth's method for predicting the effect of nozzle pressure ratio (NPR) on boattail pressure distributions. Here the predictions are compared with experimental data[33,35] obtained at a freestream Mach number of 0.8 for an $l/D=1.768$, $d_B/D=0.51$ circular arc nozzle. For this unseparated flow case, the agreement between the experiment and calculations is excellent.

Figure 5 presents a comparison of the predictions of Wilmoth's method with experiment for a nozzle configuration on which boundary-layer separation occurs. This circular arc convergent nozzle had an $l/D=0.8$ and $d_B/D=0.51$. The experimental results were obtained at $M_\infty=0.8$. For these calculations Wilmoth used the experimentally obtained location of separation.[36] The predicted pressure distributions are in good agreement with the experiment.

A comparison of predicted boattail pressure drag with experiment[33-35] is shown on Fig. 6. For the attached flow nozzle, the theory underpredicts the drag slightly but correctly predicts the trend with nozzle pressure ratio. For the nozzle with a separated boundary layer, the agreement between experiment and theory is very sensitive to the separation location. At $M_\infty=0.6$, using the Presz method for predicting separation location resulted in very good predictions of the boattail pressure drag. However, at $M_\infty=0.8$, using the separation location predicted by Presz's method resulted in an underprediction of the drag. Using the experimentally determined separation location[36] gave good results at $M_\infty=0.8$, but resulted in an underprediction of boattail pressure drag at $M_\infty=0.6$. (Note that at $M_\infty=0.6$, the Presz method predicted a separation location slightly upstream of the actual location, while at $M_\infty=0.8$, the Presz method predicted a separation location slightly downstream of the actual location.) It is apparent that further improvements in the analytical model of boundary-layer separation are required.

An additional feature of Wilmoth's theory is the capability to predict the flowfield surrounding the nozzles. Typical results are presented on Fig. 7, where comparisons of predictions with measured total pressure profiles[37] in a jet exhaust are presented. The flow conditions for this case are $M_\infty=0.8$, a nozzle pressure ratio of 5, and the total temperature of the jet approximately equal to freestream total temperature. The jet is exhausting from a convergent nozzle with a circular arc external geometry with $l/D=0.8$ and $d_B/D=0.51$. The predictions of the patched method are in good agreement with experiment. The experimental data show more mixing of the two streams than predicted. This discrepancy may be associated with the overlaid shear layer

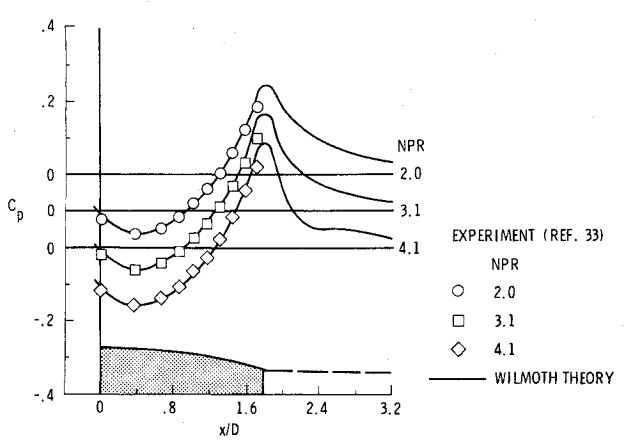

Fig. 4 Comparison of predictions of patched method with experiment for an $l/D=1.768$, $d_B/D=0.51$ circular nozzle at $M_\infty=0.8$.

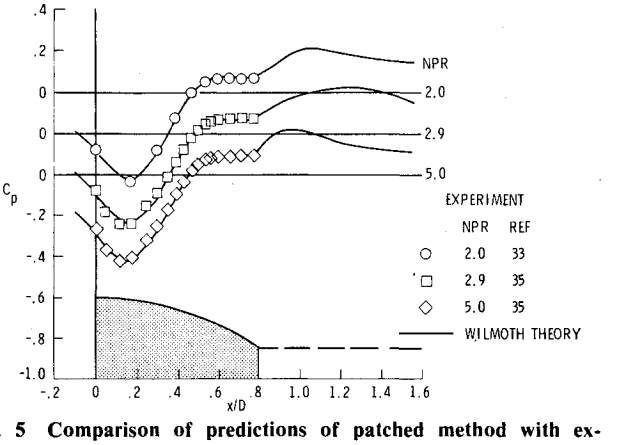

Fig. 5 Comparison of predictions of patched method with experiment for an $l/D=0.8$, $d_B/D=0.51$ circular arc nozzle at $M_\infty=0.8$.

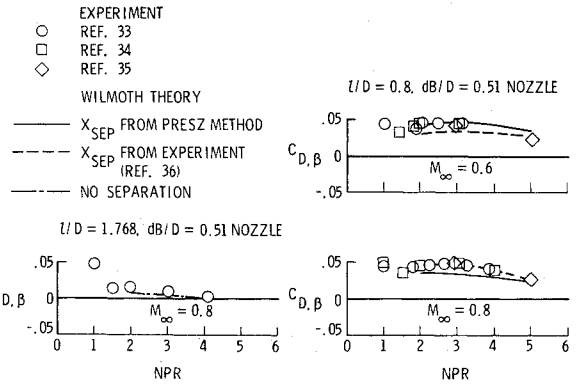

Fig. 6 Comparison of experimental and predicted boattail pressure drag for $d_B/D = 0.51$ circular arc nozzles.

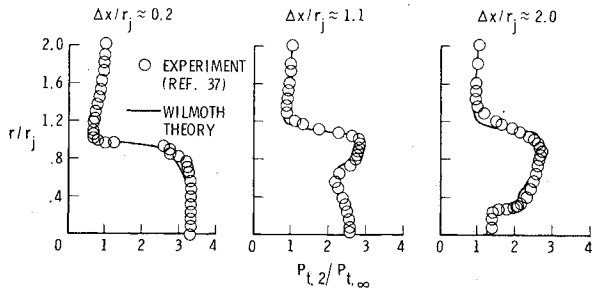

Fig. 7 Total pressure profiles in a jet exhaust from an $l/D = 0.8$, $d_B/D = 0.51$ circular arc nozzle at $M_\infty = 0.8$ and NPR = 5.0.

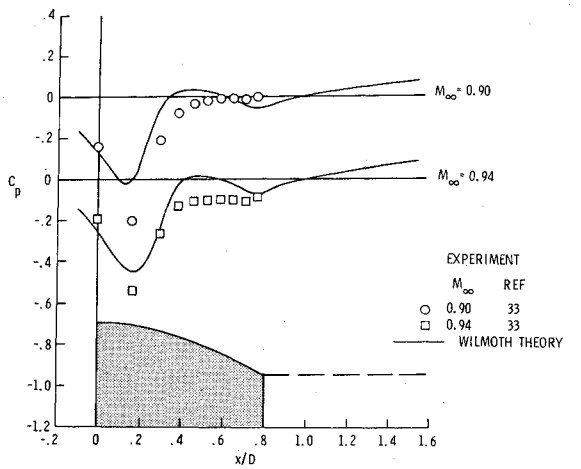

Fig. 8 Comparison of predictions of patched method with experiment for an $l/D = 0.8$, $d_B/D = 0.51$ circular arc nozzle at NPR = 2.0 and $M_\infty = 0.90$ and 0.94.

theory using a too low initial turbulence level for the jet flow or it may be associated with the turbulence model used in the mixing calculations.

When the boundary layer separates on the nozzle owing to shock waves at transonic speeds, the patched method can give very poor results. As can be seen on Fig. 8, at $M_\infty = 0.90$ and 0.94 the patched method of Wilmoth substantially overpredicts the surface pressures on the $l/D = 0.8$, $d_B/D = 0.51$ circular arc nozzle. This discrepancy is associated primarily with the analytical model of the separation region. To date, the available patched methods attempt to model this strong shock-induced viscous interaction using weak interaction theory. While the patched inviscid/viscous interaction method is capable of providing good cheap predictions of nozzle external flow characteristics at subcritical speeds, further improvements in the analytical model of the strong viscous interaction region are necessary if good predictions are to be consistently obtained at supercritical speeds.

Solutions of the Navier-Stokes Equations

Generally the elements of the Navier-Stokes codes being applied to afterbody flows are well-documented, validated computational techniques.

The Reynolds' averaged continuity, momentum, and energy equations are written in conservation-law form as

$$\frac{\partial U}{\partial t} + \frac{\partial F}{\partial z} + \frac{\partial G}{\partial r} + H = 0$$

where

$$U = r\begin{bmatrix} \rho \\ \rho u \\ \rho v \\ E \end{bmatrix} \qquad F = r\begin{bmatrix} \rho u \\ \rho u^2 - \tau_{zz} \\ \rho uv - \tau_{zr} \\ Eu - \tau_{zz}u - \tau_{zr}v + \dot{q}_z \end{bmatrix}$$

$$G = r\begin{bmatrix} \rho v \\ \rho uv - \tau_{rz} \\ \rho v^2 - \tau_{rr} \\ Ev - \tau_{rz}u - \tau_{rr}v + \dot{q}_r \end{bmatrix} \qquad H = \begin{bmatrix} 0 \\ 0 \\ \tau_{\theta\theta} \\ 0 \end{bmatrix}$$

and the mean total energy is

$$E = \rho\left(c_v T + \frac{u^2 + v^2}{2}\right)$$

The elements of the stress tensor and heat-flux vector are given by

$$\tau_{zz} = -p - \frac{2}{3}(\mu + \epsilon)\left(\frac{\partial v}{\partial r} + \frac{v}{r}\right) + \frac{4}{3}(\mu + \epsilon)\frac{\partial u}{\partial z}$$

$$\tau_{rr} = -p - \frac{2}{3}(\mu + \epsilon)\left(\frac{\partial u}{\partial z} + \frac{v}{r}\right) + \frac{4}{3}(\mu + \epsilon)\frac{\partial v}{\partial r}$$

$$\tau_{\theta\theta} = -p - \frac{2}{3}(\mu + \epsilon)\left(\frac{\partial u}{\partial z} + \frac{\partial v}{\partial r}\right) + \frac{4}{3}(\mu + \epsilon)\frac{v}{r}$$

$$\tau_{rz} = \tau_{zr} = (\mu + \epsilon)\left(\frac{\partial u}{\partial r} + \frac{\partial v}{\partial z}\right)$$

where

$$\vec{q} = -c_p\left(\frac{\mu}{P_R} + \frac{\epsilon}{P_{R,t}}\right)\nabla T$$

The coefficient of molecular viscosity, μ, is given by Southerland's relation, and the eddy viscosity, ϵ, is usually given by an algebraic mixing length model. The specification of an equation of state for the gas, usually the perfect gas model, completes the system of equations.

The governing Navier-Stokes equations are numerically solved in a transformed computational x,y plane. The governing equations in the computational plane can be written as

$$\frac{\partial U}{\partial t} + x_z\frac{\partial F}{\partial x} + x_r\frac{\partial G}{\partial x} + y_z\frac{\partial F}{\partial y} + y_r\frac{\partial G}{\partial y} + H = 0$$

The derivatives in the definitions of the components of the stress tensor and heat-flux vector are expanded in the same manner. The transformation derivatives x_z, x_r, y_z, and y_r are determined from the relations

$$x_z = Jr_y \qquad y_z = -Jr_x \qquad x_r = -Jz_y \qquad y_r = Jz_x$$
$$J = x_z y_r - x_r y_z = 1/(z_x r_y - z_y r_x)$$

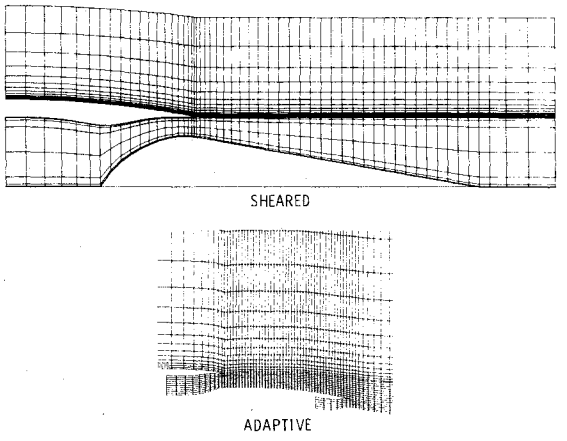

Fig. 9 Finite-difference grids in the physical domain used in solutions of the Navier-Stokes equations.

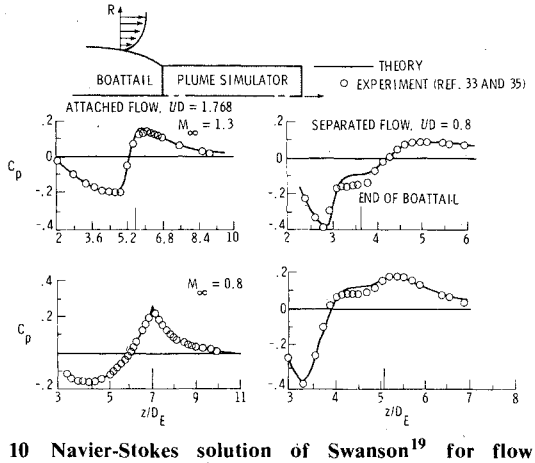

Fig. 10 Navier-Stokes solution of Swanson[19] for flow over $d_B/D = 0.51$ circular arc boattail nozzles with solid plume simulators.

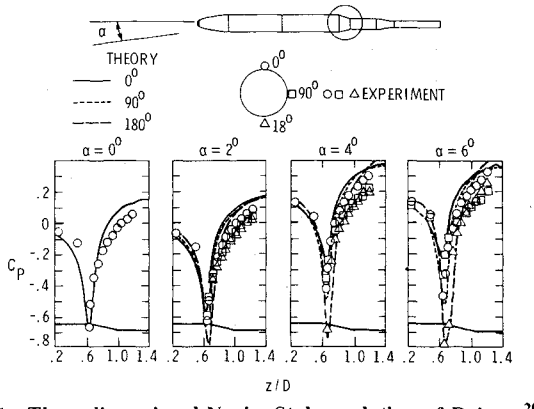

Fig. 11 Three-dimensional Navier-Stokes solution of Deiwert[20] for flow over afbodies at angle of attack and $M_\infty = 0.9$.

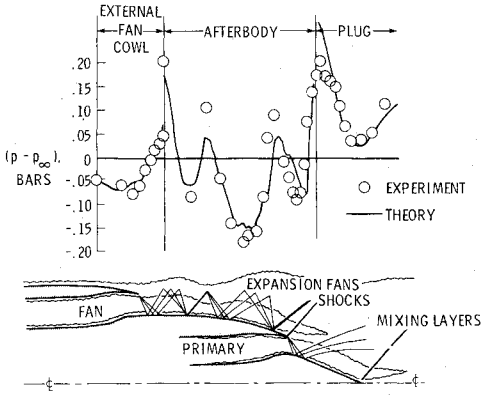

Fig. 12 Navier-Stokes solution of Peery and Forester[18] for multistream exhaust nozzle flow. NPR = 2.6 and $M_\infty = 0.9$.

where the subscripts indicate partial differentiation, and where J is the transformation Jacobian. The derivatives are computed numerically.

Several algorithms are being used to solve the governing equations. The most widely used algorithm is the explicit predictor-corrector finite-difference scheme of MacCormack.[38] This algorithm results in robust codes which are efficient on vector processors. The implicit method of Beam and Warming[39] using approximate factorization of the algorithm operators is also being used to solve the governing equations. Fourth-order dissipation terms[40] are added explicitly to both methods in order to produce stable shock wave transitions.

The computational grids used for afterbody jet flows generally have been either a sheared grid[15-17,19,24] or an adaptive grid,[18,23,25] (see Fig. 9). The sheared grid provides good resolution in the high gradient regions of the boundary layer, but may not necessarily provide good resolution in the high gradient regions of the jet-mixing layer. The adaptive grid allows a fine mesh region to remain in the high gradient mixing layer between the jet and freestream flow as the solution tends towards convergence. The streamwise grid lines are generally aligned with the afterbody and jet streamlines and are clustered in the body boundary layers and mixing layers. The transverse or radial grid lines are generally normal to the body axis and clustered in the afterbody and near-jet regions. Multistream exhaust nozzle flows have been computed[18] with the adaptive grid. Each stream has its own computational region partially bounded by the adaptive streamwise grid lines.

The Navier-Stokes equations are parabolic in time and elliptic in space and hence require initial conditions and boundary conditions to be specified for the solution domain. The initial conditions are usually specified by less complex methods such as patched solution procedures or parabolized Navier-Stokes solutions. Boundary conditions vary according to whether the flow at the boundary point in question is subsonic or supersonic. For inflow boundary points, total pressure and temperature along with flow angularity are specified for subsonic points, while all velocities and thermodynamic variables are specified for supersonic points. Subsonic outflow boundaries have only static pressure prescribed and, at a supersonic outflow, boundary variables are usually extrapolated. Symmetry is enforced on the centerline while uniform freestream conditions are imposed on the far-field lateral boundaries.

The transport of momentum and energy by turbulence is implemented through local eddy viscosity models. The two-layer algebraic models of Cebeci and Smith[41] or Baldwin and Lomax[42] are in general use for the afterbody boundary layers. The relaxation eddy viscosity model of Shang and Hankey[43] has been applied with reasonable success to separated afterbody flows and approximates the relaxation of turbulence from sudden disturbances towards equilibrium. In the mixing layer between the jet and freestream, the eddy viscosity is represented by a mixing length model[18] where the length scale is taken to be the width of the mixing layer. Much research is still required to experimentally and computationally formulate proper turbulence models for the complex afterbody/jet flows.

Numerical solutions of the Navier-Stokes equations are currently finding applications in a number of afterbody flow analysis and design procedures. The experimentally based nozzle design approach is well understood but tends to limit the design space. This approach can result in suboptimal configurations in addition to being increasingly expensive.

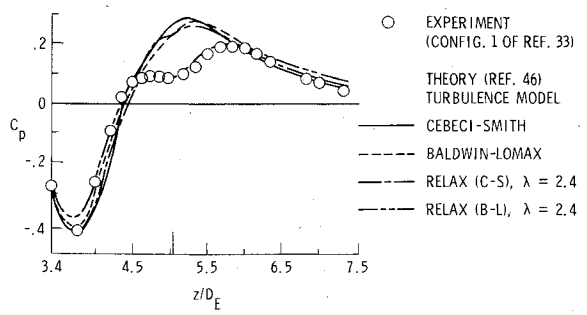

Fig. 13 Effect of algebraic eddy viscosity model on flow over an $l/D=0.8$, $d_B/D=0.51$ aftbody at $M_\infty=0.8$ as shown by Swanson in Ref. 45.

Numerical simulations of nozzle flows are being used to augment experimental data bases or to aid in investigation of anomalies in afterbody performance. Government and industry are currently active in developing, validating, and using these codes as they will play a large role in afterbody design, test, and evaluation in the near future.

Application of the Navier-Stokes codes to axisymmetric afterbodies is illustrated in Fig. 10. The computations were performed by Swanson[19] on the NASA Langley CYBER 203 computer. The analyses are simulations of attached and separated flows over circular arc boattails with solid plume simulators.[33] The computed pressure distributions agree well with the data except in the separated regions, where the pressure is overpredicted. The supersonic solutions require 5 min, whereas corresponding subsonic solutions require from 1.5 to 2.5 hours to obtain convergence.

Three-dimensional solutions of the Navier-Stokes equations for afterbodies have been obtained by Deiwert[20] and Thomas.[22] Flowfields about axisymmetric boattail bodies at angle of attack with solid plume simulators have been computed by Deiwert. Figure 11 shows a comparison of a boattail surface pressure between the solution and the experimental data[44] at angles of attack from 0 to 6 deg for transonic flow. The three-dimensional flow characteristics are simulated quite well. For these solutions the thin shear layer approximation to the Navier-Stokes equations was solved using an implicit algorithm on the NASA Ames ILLIAC IV computer.

Multistream nozzle solutions have been numerically simulated with the Navier-Stokes methods. These solutions[18,23] represent significant applications of the Navier-Stokes methods to nozzle design and augmentation of experimental data bases. As an example of this capability, the axisymmetric flowfield about a scale model of JT9D turbofan engine was calculated as shown in Fig. 12 at a nozzle pressure ratio of 2.6 and a freestream Mach number of 0.9. The computed static pressures on the three external nozzle surfaces are compared with measured pressures in Fig. 12. The agreement between the calculated and measured pressures is good. This solution required 30 min on a CYBER 175 computer. Note that Refs. 18 and 23 use wall functions and free slip boundary conditions on the nozzle surfaces which substantially reduce the computation time required.

The Navier-Stokes computations of afterbody flows are not yet the panacea they might appear. Much work, numerically and experimentally, needs to be accomplished. Validation of the codes is being hindered by the lack of detailed experimental data. The complexity of the nozzle flowfield, such as severe pressure gradients, mixing layers, shock-boundary-layer-induced separations, and three-dimensional flows, makes the acquisition and understanding of experimental data a formidable task. Numerically, faster solution algorithms and better turbulence models are needed. An example of the importance of properly modeling the Reynolds' stresses was demonstrated by Swanson.[45] These Navier-Stokes calculations for separated boattail flows using various eddy viscosity models are shown in Fig. 13 and compared with the experimental data of Reubush.[33] At subsonic conditions, the algebraic eddy viscosity models of Cebeci and Smith and Baldwin and Lomax yield similar results of predicting the expansion well but not reproducing the pressure plateau in the separated region. The use of the relaxation method of Shang and Hankey (relaxation initiated just upstream of separation) with the Cebeci-Smith model produces little change in the pressure distribution over the basic Cebeci-Smith model. However, by using the relaxation method in conjunction with the Baldwin-Lomax eddy viscosity model, the separation region plateau pressure is simulated properly but the expansion region pressure is not reproduced well. Similar anomalies occur at supersonic conditions between the various eddy viscosity models.

Concluding Remarks

As a result of an extensive analytical development, many methods are available today for predicting the pressure distribution and drag of axisymmetric nozzle aftbody configurations. These methods vary in complexity from empirical procedures to solutions of the Navier-Stokes equations.

The patched inviscid/viscous interaction technique provides good predictions of nozzle pressure distributions, nozzle pressure drag, and flowfield characteristics at reasonable cost. However, this technique does not consistently give good results when strong viscous interactions and/or shock waves are present. Significant improvements in the analytical model of separated flow used in these procedures are needed.

Numerical solutions of the Navier-Stokes equations for afterbody flows are being reported in the literature with increasing regularity. In principle, these methods may be used to compute complex interacting flows around three-dimensional aftbodies. Currently, the use of Navier-Stokes in nozzle aftbody flow analysis is being paced by the flow turbulence modeling, the data storage requirements, and the cost of performing the computations. In spite of these hinderances, measurable progress has been made and there is considerable interest in applying Navier-Stokes codes in nozzle design to offset the increasing cost of experimental testing.

References

[1]Rom, J. and Bober, L.J., "Calculation of the Pressure Distribution on Axisymmetric Boattails Including Effects of Viscous Interactions and Exhaust Jets in Subsonic Flow," NASA TM X-3109, 1974.

[2]Chow, W.L., Bober, L.J., and Anderson, B.H., "Numerical Calculation of Transonic Boattail Flow," NASA TN D-7984, 1975.

[3]Reubush, D.E. and Putnam, L.E., "An Experimental and Analytical Investigation of the Effect on Isolated Boattail Drag of Varying Reynolds Number up to 130×10^6," NASA TN D-8210, 1976.

[4]Wilmoth, R.G., "Computation of Transonic Boattail Flow with Separation," NASA TP-1070, 1977.

[5]Cosner, R.R. and Bower, W.W., "A Patched Solution of the Transonic Flowfield About an Axisymmetric Boattail," AIAA Paper 77-227, Jan. 1977.

[6]Yaeger, L.S., "Transonic Flow Over Afterbodies Including the Effects of Jet-Plume and Viscous Interactions With Separation," AIAA Paper 77-228, Jan. 1977.

[7]Yaros, S.F., "An Analysis of Transonic Viscous/Inviscid Interactions on Axisymmetric Bodies With Solid Stings or Real Plumes," AEDC-TR-77-106, Feb. 1978 (available from DTIC and AD A050 401).

[8]Presz, W.M. Jr., King, R.W., and Buteau, J.D., "An Improved Analytical Model of the Separated Region on Boattail Nozzles at Subsonic Speeds," NASA CR-3028, 1978.

[9]Kuhn, G.D., "Calculation of Separated Turbulent Flows on Axisymmetric Afterbodies Including Exhaust Plume Effects," AIAA Paper 79-0303, 1979.

[10]Wilmoth, R.G., "RAXJET: A Computer Program for Predicting Transonic Axisymmetric Flow Over Nozzle Afterbodies with Supersonic Jet Exhausts," NASA TM-83235, Feb. 1982.

[11]Putnam, L.E., "DONBOL: A Computer Program for Predicting Axisymmetric Nozzle Afterbody Pressure Distributions and Drag at Subsonic Speeds," NASA TM-78779, 1979.

[12]Kuhn, G.D., "An Improved Interaction Method for Calculating Exhaust Nozzle Boattail Flows," AEDC TR-80-19, Oct. 1980.

[13]Carter, J.E., "Viscous-Inviscid Interaction Analysis of Transonic Turbulent Separated Flow," AIAA Paper 81-1241, June 1981.

[14]Cosner, R.R., "Fast Navier-Stokes Solution of Transonic Flowfield About Axisymmetric Afterbodies," AIAA Paper 80-0193, Jan. 1980.

[15]Holst, T.L., "Numerical Solution of Axisymmetric Boattail Fields with Plume Simulators," AIAA Paper 77-224, Jan. 1977.

[16]Mikhail, A.G., Hankey, W.L., and Shang, J.S., "Computation of a Supersonic Flow Past an Axisymmetric Nozzle Boattail with Jet Exhaust," AIAA Paper 78-993, July 1978.

[17]Jacocks, J.L., "Computation of Axisymmetric Separated Nozzle-Afterbody Flow," AEDC-TR-79-71, Jan. 1980 (available from DTIC as AD A079 694).

[18]Peery, K.M. and Forester, C.K., "Numerical Simulation of Multistream Nozzle Flows," AIAA Paper 79-1549, July 1979.

[19]Swanson, R.C. Jr., "Numerical Solutions of the Navier-Stokes Equations for Transonic Afterbody Flows," NASA TP-1784, Dec. 1980.

[20]Deiwert, G.S., "Numerical Simulation of Three-Dimensional Boattail Afterbody Flow Fields," AIAA Paper 80-1347, July 1980.

[21]Thomas, P.D., "Numerical Method for Prediction Flow Characteristics and Performance of Nonaxisymmetric Nozzles—Theory," NASA CR-3147, 1979.

[22]Thomas, P.D., "Numerical Method for Predicting Flow Characteristics and Performance of Nonaxisymmetric Nozzles—Applications," NASA CR-3264, 1980.

[23]Perry, K.M. and Russell, D.L., "A Numerical Investigation of Exhaust Plume Temperature Effects on Nonaxisymmetric Nozzle/Afterbody Performance," AGARD Symposium on Aerodynamics of Power Plane Installations, AGARD CP-301, May 1981.

[24]Cline, M.C. and Wilmoth, R.G., "Computation of High Reynolds Number Internal/External Flows," AIAA Paper 81-1194, June 1981.

[25]Hasen, G.A., "Navier-Stokes Solutions for an Axisymmetric Nozzle," AIAA Paper 81-1474, 1981.

[26]South, J.C. Jr. and Jameson, A., "Relaxation Solutions for Inviscid Axisymmetric Transonic Flow Over Blunt or Pointed Bodies," *Proceedings of the AIAA Computational Fluid Dynamics Conference*, July 1973, pp. 8-17.

[27]Keller, J.D. and South, J.C. Jr., "RAXBOD: A FORTRAN Program for Inviscid Transonic Flow Over Axisymmetric Bodies," NASA TM X-72831, 1976.

[28]Dash, S.M. and Thorpe, R.D., "A New Shock-Capturing/Shock-Fitting Computational Model for Analyzing Supersonic Inviscid Flows (the SCIPPY Code)," Report No. 366, Aeronautical Research Association of Princeton, Inc., Nov. 1978.

[29]Reshotko, E. and Tucker, M. "Approximate Calculation of the Compressible Turbulent Boundary Layer with Heat Transfer and Arbitrary Pressure Gradient," NACA TN-4154, 1957.

[30]*Users Manual for the External Drag and Internal Nozzle Performance Deck (Deck XI)—Supersonic Flow Analysis (Applicable to Deck VI)*. PWA-3464, Suppl. F, Pt. I [Contract AF33(615) 3128], Pratt and Whitney Aircraft, Sept. 1968.

[31]Dash, S.M. and Pergament, H.S., "A Computational Model for the Prediction of Jet Entrainment in the Vicinity of Nozzle Boattails (the BOAT Code)," NASA CR-3075, 1978.

[32]Dash, S.M., Wilmoth, R.G., and Pergament, H.S., "Overlaid Viscous Inviscid Model for the Prediction of Near-Field Jet Entrainment," *AIAA Journal*, Vol. 17, Sept. 1979, pp. 950-958.

[33]Reubush, D.E., "Experimental Study of the Effectiveness of Cylindrical Plume Simulators for Predicting Jet-On Boattail Drag at Mach Numbers up to 1.30," NASA TN D-7795, 1974.

[34]Reubush, D.E. and Runckel, J.F., "Effect of Fineness Ratio on the Boattail Drag of Circular-Arc Afterbodies Having Closure Ratios of 0.50 with Jet Exhaust at Mach Numbers Up to 1.30," NASA TN D-7192, 1973.

[35]Abeyounis, W.K. and Putnam, L.E., "Investigation of the Flow Field Surrounding Circular-Arc Boattail Nozzles at Subsonic Speeds," NASA TP-1633, 1980.

[36]Abeyounis, W.K., "Boundary-Layer Separation on Isolated Boattail Nozzles," NASA TP-1226, 1978.

[37]Mason, M.L. and Putnam, L.E., "Pitot Pressure Measurements in Flow Fields Behind Circular-Arc Nozzles with Exhaust Jets at Subsonic Free-Stream Mach Numbers," NASA TM-80169, 1979.

[38]MacCormack, R.W., "The Effect of Viscosity in Hypervelocity Impact Cratering," AIAA Paper 69-354, April-May 1969.

[39]Beam, R. and Warming, R.F., "An Implicit Finite Difference Algorithm for Hyperbolic Systems Conservation-Law-Form," *Journal of Computational Physics*, Vol. 22, Sept. 1976, pp. 87-110.

[40]MacCormack, R.W. and Baldwin, B.S., "A Numerical Method for Solving the Navier-Stokes Equations with Application to Shock-Boundary Layer Interactions," AIAA Paper 74-603, June 1974.

[41]Cebeci, T., Smith, A.M.O., and Mosinskis, G., "Calculation of Compressible Adiabatic Turbulent Boundary Layers," *AIAA Journal*, Vol. 8, Nov. 1970, pp. 1974-1982.

[42]Baldwin, B. and Lomax, H., "Thin-Layer Approximation and Algebraic Model for Separated Turbulent Flows," AIAA Paper 78-257, Jan. 1978.

[43]Shang, J.S. and Hankey, W.L. Jr., "Numerical Solution for Supersonic Turbulent Flow Over a Compression Ramp," *AIAA Journal*, Vol. 13, Oct. 1975, pp. 1368-1374.

[44]Shrewsbury, G.D., "Effect of Boattail Juncture Shape on Pressure Drag Coefficients of Isolated Afterbodies," NASA TM X-1517, 1968.

[45]Staff of the Langley Research Center, "A Compendium of Computational Fluid Dynamics at the Langley Research Center," NASA TM X-81877, 1980.